Supporting Information

π-π Interactions Modulate Charge Transport in Peptide-Based Frameworks

Liwen Su, Yongkang Zhang, Pan Qi, Han Liang, Huili Wang, and Cunlan Guo[*]

College of Chemistry and Molecular Sciences, Wuhan University, Wuhan, Hubei 430072, P. R. China

Email: cunlanguo@whu.edu.cn

Table of contents

1. Experimental section

1.1 Chemical reagents

All peptides with a mercaptopropionic acid (MPA) linker at the N-terminus with purity > 95% (HPLC) were purchased from GL Biochem. and stored at -20 °C. Deionized water (18.2 MΩ·cm) was purified by using PURELAB Ultra from ELGA LabWater company. N-(3-Dimethylaminopropyl)-N'-ethylcarbodiimide hydrochloride (EDC) and Eutectic gallium-indium (EGaIn) (purity ≥ 99.99%) were purchased from Sigma-Aldrich. 1-Methyl-1'-aminoethyl-4,4'-bipyridinium salt (MV^{2+}) was synthesized according to the methods in the literature.[1] The optical adhesive was purchased from Norland (NOA 61). All chemical reagents were used as obtained unless stated otherwise.

1.2 Preparation of template-stripped gold substrate

The ultra-flat gold substrates (Au^{TS}) were prepared by the template-stripped method.[2, 3] First, the Si wafer was cleaned by sonication in deionized water, acetone, and isopropyl alcohol for 5 minutes, respectively. Then, the cleaned Si wafer was treated by plasma for 3 minutes under 1:1 Ar and O_2, and etched by 2% HF for 2 minutes. After one repetition, the Si wafer was treated by plasma under O_2 for 10 minutes. Next, a 100 nm gold film was evaporated on the Si wafer by a thermal evaporator. The cleaned glass slides (~1 × 1 cm^2) were glued on the gold film by curing the optical adhesive under UV light for 4 hours. The fresh Au substrates were stripped from the Si wafer and immediately used for the following preparation of peptide and peptide-MV^{2+} SAMs.

2. Surface coverage

The surface coverage of peptide-MV^{2+} SAMs was determined by CV. The general equation applied to determine the surface coverage (Γ') of redox molecules such as MV^{2+} was as follows (eq. 1).

$$\Gamma' = \frac{Q}{nFA} \qquad \text{(eq. 1)}$$

where Q is the charge passed for the reduction or the oxidation process. Q could be extracted by integrating the area under the CV peaks. n is the number of electrons per mol of reaction, F is the Faraday constant, and A is the area of the electrode.

## 3. Landauer formula

To evaluate the J-V behaviors through peptide and peptide-MV^{2+} SAMs, we fitted the experimental J-V data ranging from −0.5 to +0.5 V based on the Landauer formula (eq. 2).[4]

$$I \cong N \frac{2e}{h} \Gamma_g^2 \frac{eV}{(\delta E + \alpha eV)^2 - (eV/2)^2} \qquad \text{(eq. 2)}$$

where δE is the energy difference between the closest orbital energy of the peptide SAMs (HOMO or LUMO) and the Fermi level of the electrode. Γ_g is the molecule-electrode coupling. h is the Plank's constant, e is the charge of an electron, α is the asymmetric factor, and N is the effective number of molecules participating in the current. The value of N was uniformly set to 4.08×10^9, from our published data,[5, 6] which was an empirical value.

Figures and tables
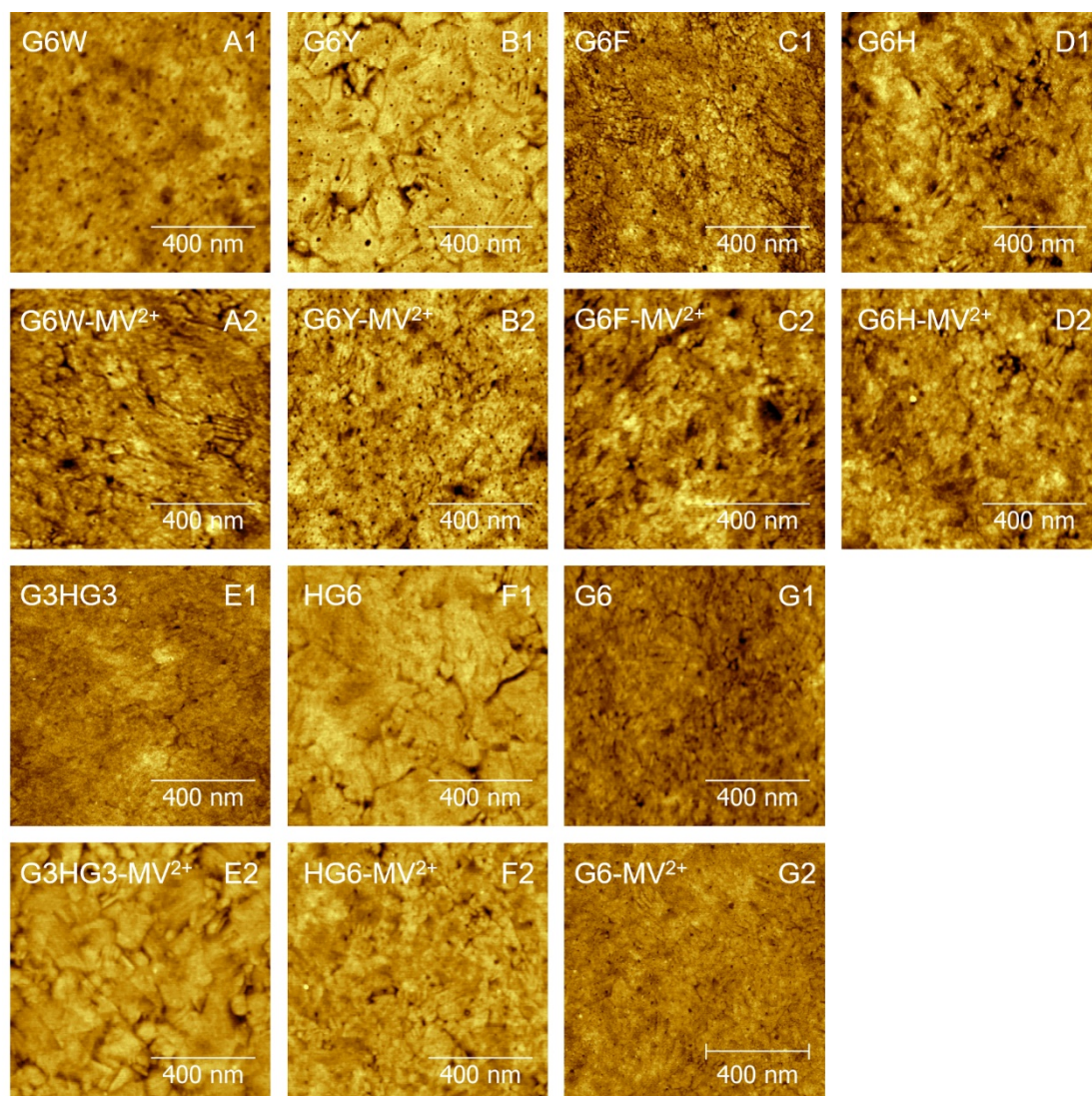
Fig. S1 Surface topographies of peptide (A1-G1) and peptide-MV^{2+} (A2-G2) SAMs measured by AFM imaging. (A1) G6W, (B1) G6Y, (C1) G6F, (D1) G6H, (E1) G3HG3, (F1) HG6, and (G1) G6 SAMs; (A2) G6W-MV^{2+}, (B2) G6Y-MV^{2+}, (C2) G6F-MV^{2+}, (D2) G6H-MV^{2+}, (E2) G3HG3-MV^{2+}, (F2) HG6-MV^{2+}, and (G2) G6-MV^{2+} SAMs.
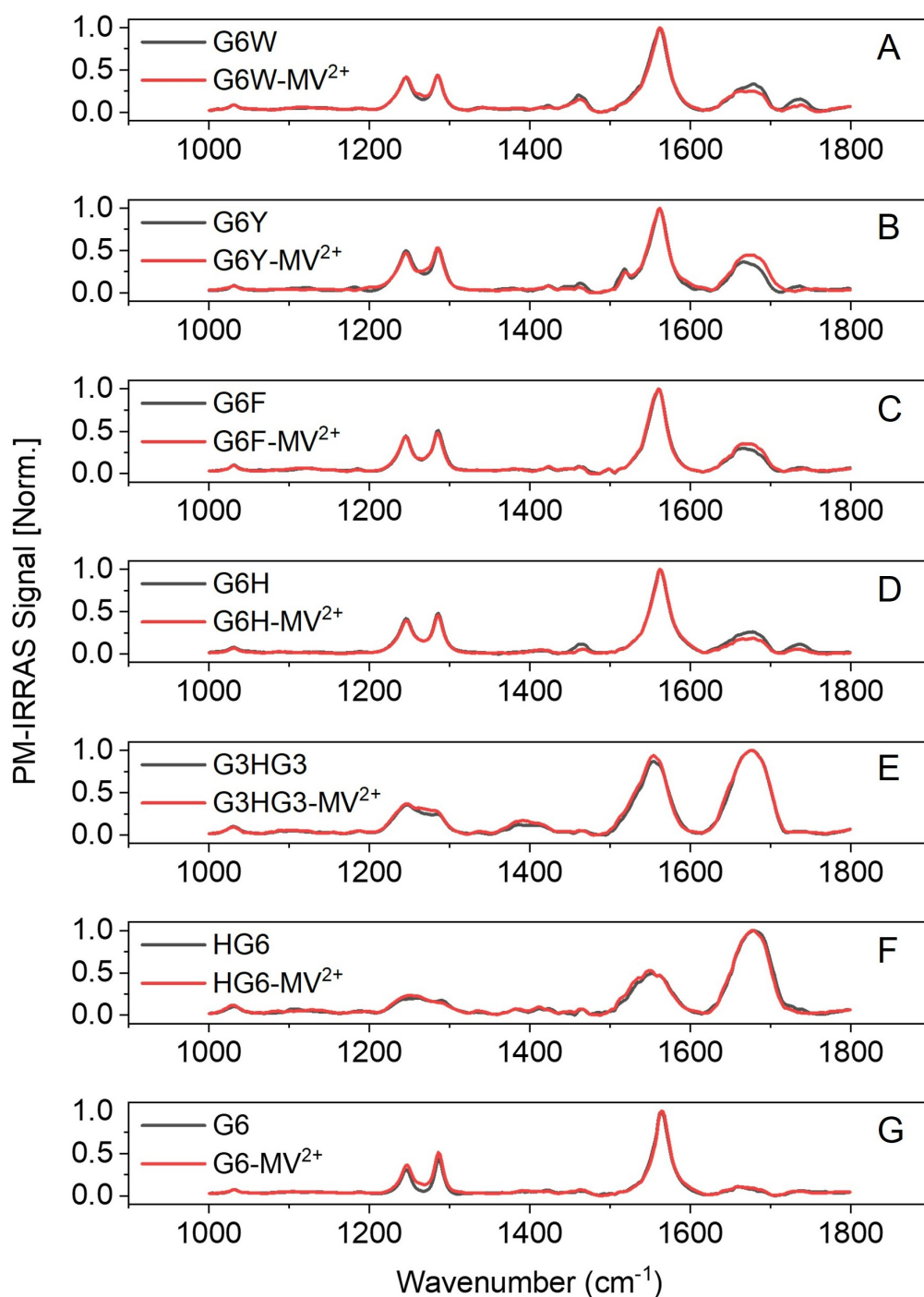
Fig. S2 Normalized PM-IRRAS spectra of the peptide and peptide-MV^{2+} SAMs with 4 cm^{-1} band resolution in the range of 1000-1800 cm^{-1}. (A) G6W and G6W-MV^{2+} SAMs, (B) G6Y and G6Y-MV^{2+} SAMs, (C) G6F and G6F-MV^{2+} SAMs, (D) G6H and G6H-MV^{2+} SAMs, (E) G3HG3 and G3HG3-MV^{2+} SAMs, (F) HG6 and HG6-MV^{2+} and (G) G6 and G6-MV^{2+} SAMs. The black and red curves show the IR curves of the peptide and peptide-MV^{2+} SAMs, respectively.

As seen from the normalized PM-IRRAS spectra of peptide SAMs, the amide I/II ratios were similar for peptide-based SAMs with aromatic amino acid residues on the top (Fig. S2A-D). Combined with the AFM morphology characterizations and ellipsometry thickness measurements, the dense and uniform peptide SAMs with similar thicknesses between 28-32 Å were constructed on a gold surface.

Combining the morphology from AFM and thickness from ellipsometry, we have also constructed well-defined peptide SAMs with His located at the C-terminus, in the middle, and at the N-terminus. However, the amide I/II ratios in PM-IRRAS decreased with the His moving from N- to C-terminus (Fig. S2D-F). Similar phenomena on peptide SAMs with peptide side chains at changed locations have been reported for tryptophan-doped hepta-alanine peptide SAMs[7], tyrosine-doped hepta-alanine peptide SAMs[8], and lysine-doped hepta-glycine peptide SAMs[5]. This indicates a certain bending of the peptide backbone in SAMs. For example, the G3HG3 molecule on the gold substrate tends to bend and does not have a fully stretched conformation at the micro level compared to G6H, which makes the side chain of His also have the chance to be near the top of the G3HG3 SAM and could have π-π interactions with MV^{2+}. Meanwhile, the fractions of MV^{2+} bound to the peptide SAMs were all less than 10% (Table S3). The number of molecules capable of His-MV^{2+} π-π interactions is relatively limited. This results in similar His-MV^{2+} π-π interaction strengths in MV^{2+}-bound G3HG3 and G6H SAMs.
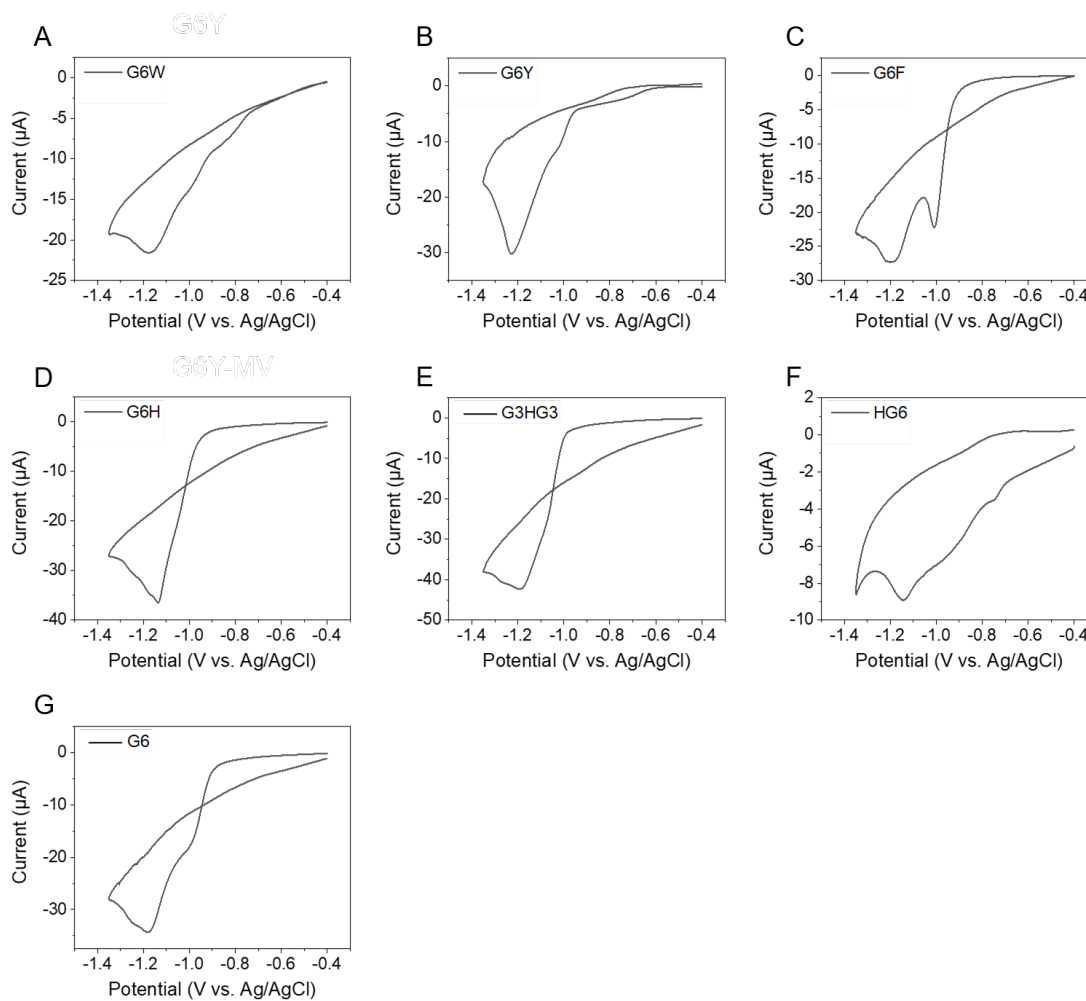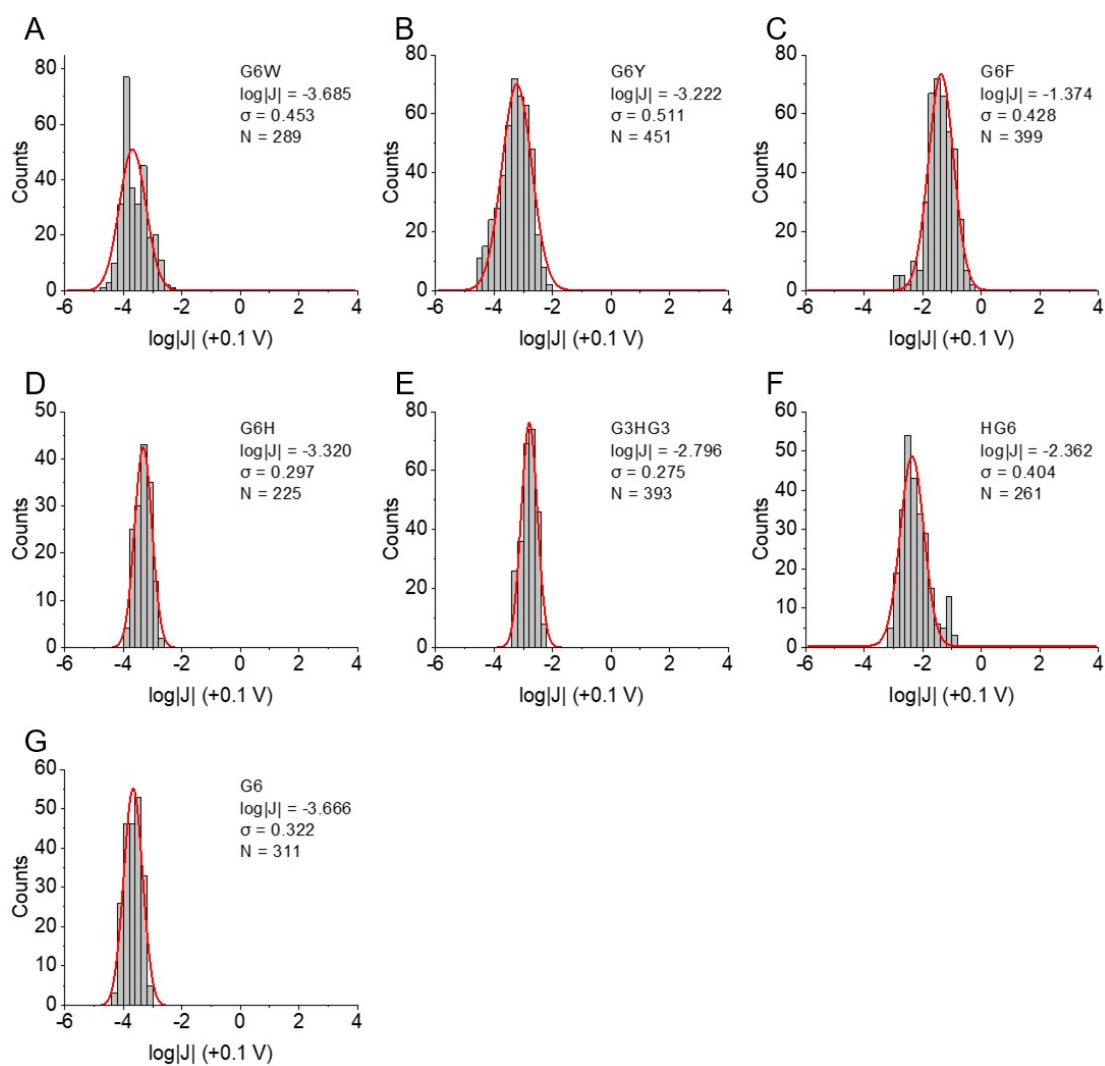
Fig. S3 CV graphs of (A) G6W, (B) G6Y, (C) G6F, (D) G6H, (E) G3HG3 (F) HG6 and (G) G6 peptide SAMs in 0.1 mol/L NaOH. Scan rate: 0.1 V/s.
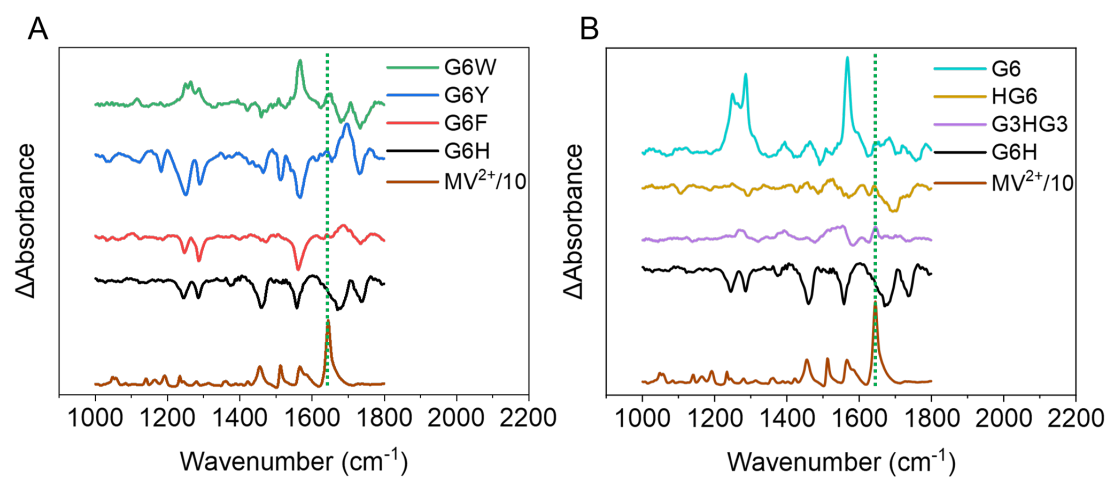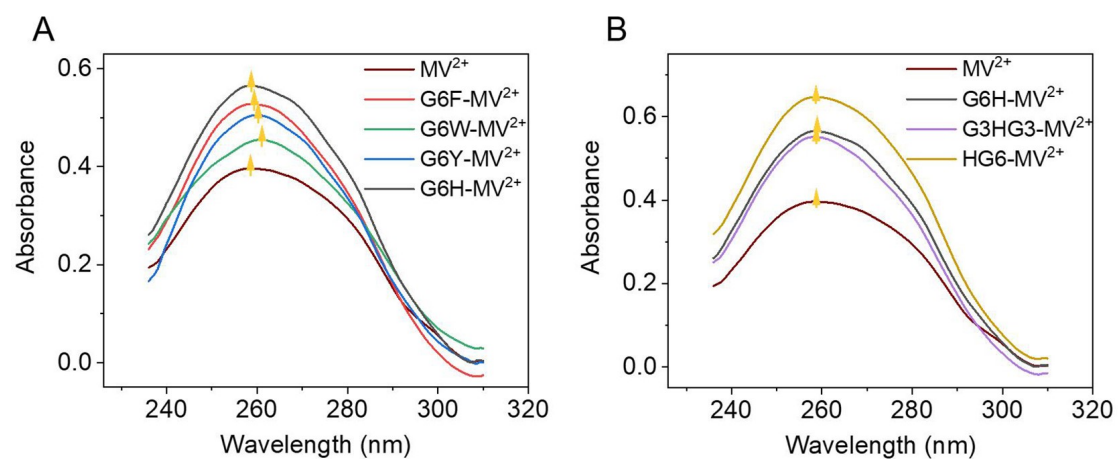
Fig. S4 PM-IRRAS difference spectrum of (A) peptide-based SAMs with aromatic amino acid residues on the top and (B) peptide-based SAMs with His located at the C-terminus, in the middle, and at N-terminus and G6-based SAM with 4 cm^{-1} band resolution in the range of 1000-1800 cm^{-1}. ΔAbsorbance= A $_{\text{peptide-MV}^{2+}}-$A $_{\text{peptide}}$. PM-IRRAS spectrum of MV^{2+} (MV^{2+}/10: divided by 10, the wine color) is shown as a reference.

Fig. S5 log|J| distribution histograms of peptide SAM junctions at +0.1 V. (A) G6W, (B) G6Y, (C) G6F, (D) G6H, (E) G3HG3, (F) HG6, and (G) G6 SAMs. The red curves represent the Gaussian fits to these histograms. All J-V measurements were performed at room temperature.
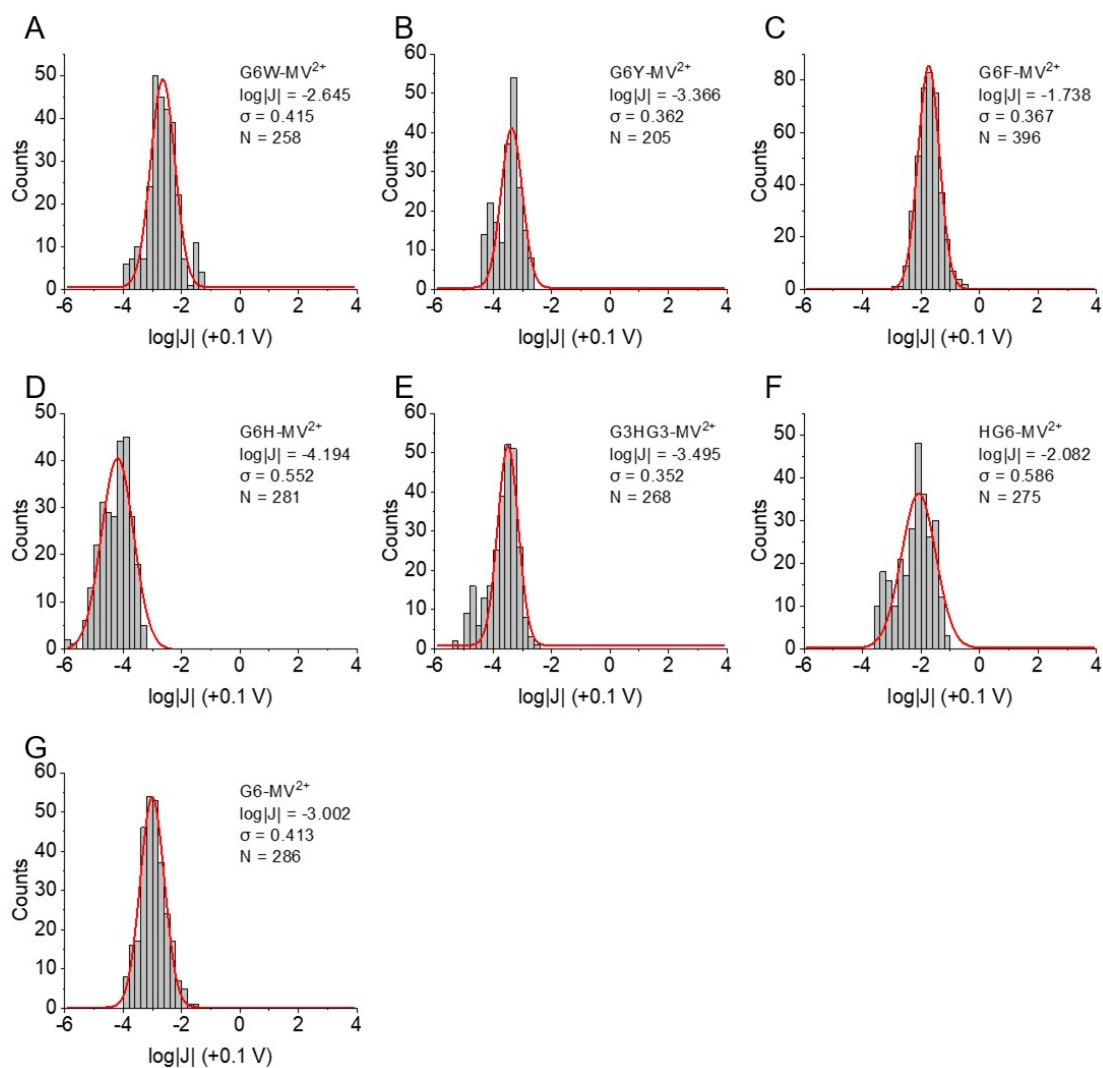
Fig. S6 log|J| distribution histograms of peptide-MV^{2+} SAM junctions at +0.1 V. (A) G6W-MV^{2+}, (B) G6Y-MV^{2+}, (C) G6F-MV^{2+}, (D) G6H-MV^{2+}, (E) G3HG3-MV^{2+}, (F) HG6-MV^{2+}, and (G) G6-MV^{2+} SAMs. The red curves represent the Gaussian fits to these histograms. All J-V measurements were performed at room temperature.

Fig. S7 Differential UV-visible spectroscopy of MV^{2+} and peptide-MV^{2+}. $A_{Peptide-MV^{2+}}$ is the difference in absorption between peptide-MV^{2+} and peptide. (A) Peptide with aromatic amino acid residues on the top and (B) peptide with His located at the C-terminus, in the middle, and at N-terminus.
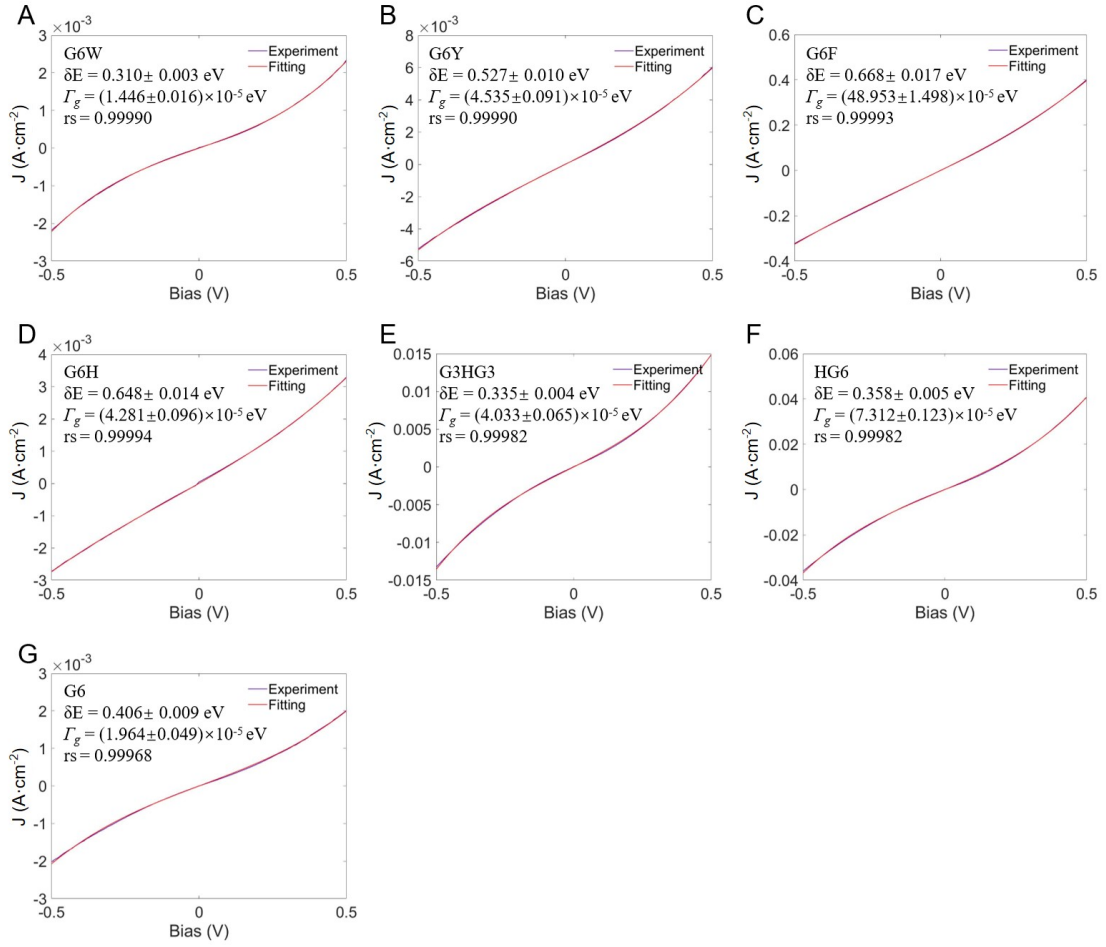
Fig. S8 J-V curve fitting for peptide SAM junctions by Landauer model. (A) G6W, (B) G6Y, (C) G6F, (D) G6H, (E) G3HG3, (F) HG6, and (G) G6 SAMs. Experimental data are in blue and fitting results are in red. Molecule-electrode energy barrier height (δE) and the energy level broadening (Γ_g) are extracted from the fitting.
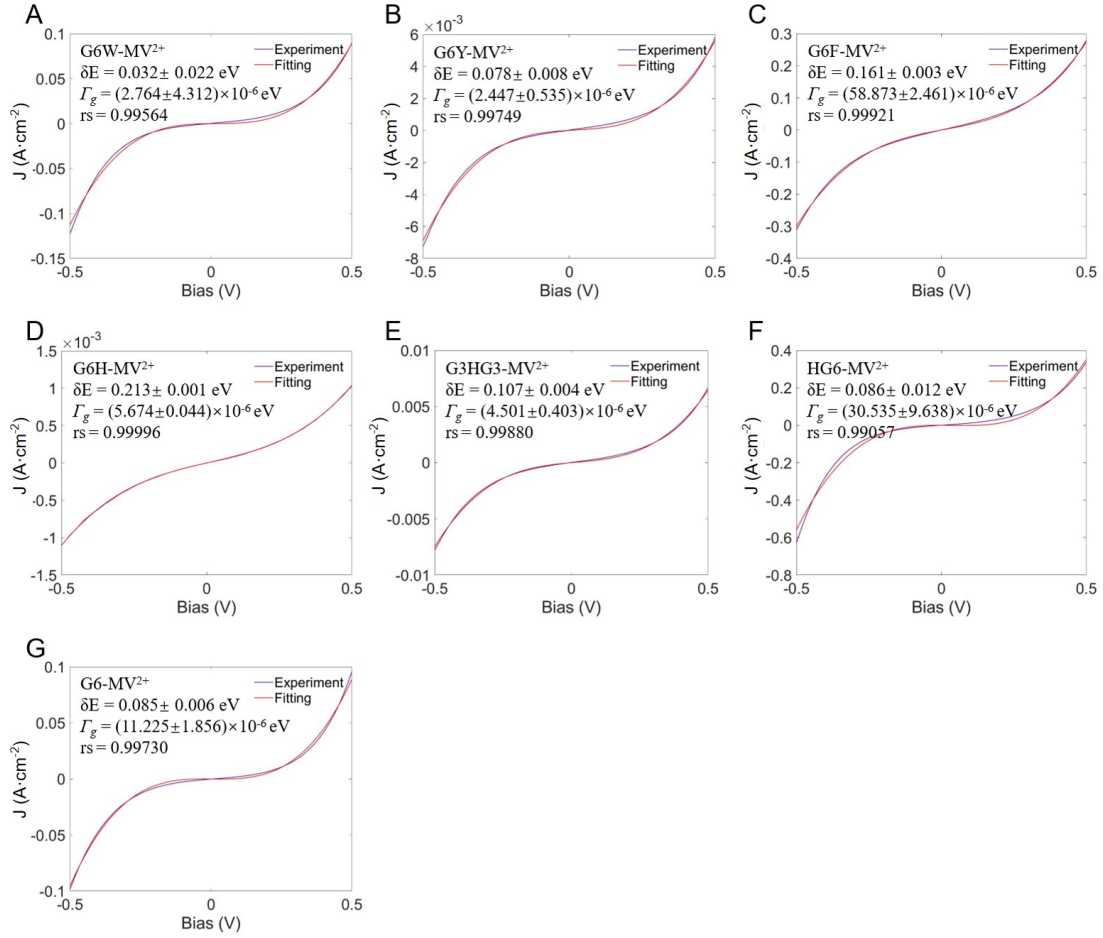
Fig. S9 J-V curve fitting for peptide-MV^{2+} SAM junctions by Landauer model. (A) G6W-MV^{2+}, (B) G6Y-MV^{2+}, (C) G6F-MV^{2+}, (D) G6H-MV^{2+}, (E) G3HG3-MV^{2+}, (F) HG6-MV^{2+}, and (G) G6-MV^{2+} SAMs. Experimental data are in blue and fitting results are in red. Molecule-electrode energy barrier height (δE) and the energy level broadening (Γ_g) are extracted from the fitting.
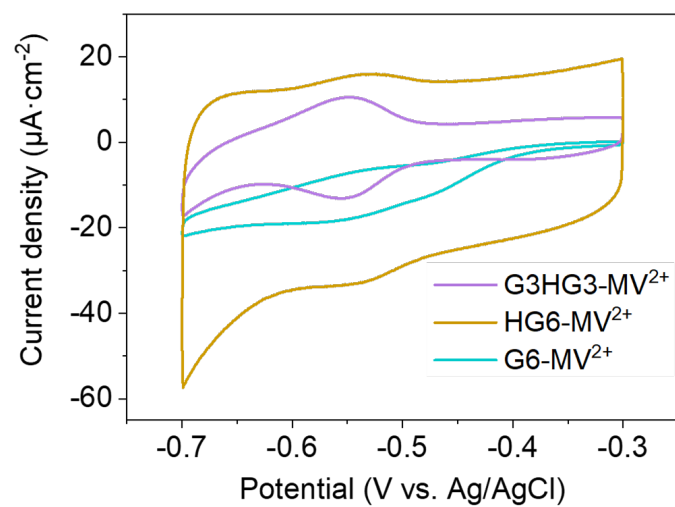
Fig. S10 CV graphs of G3HG3-MV^{2+}, HG6-MV^{2+} and G6-MV^{2+} SAMs at a scan rate of 100 mV/s in 0.1 M PB (pH = 7.0).
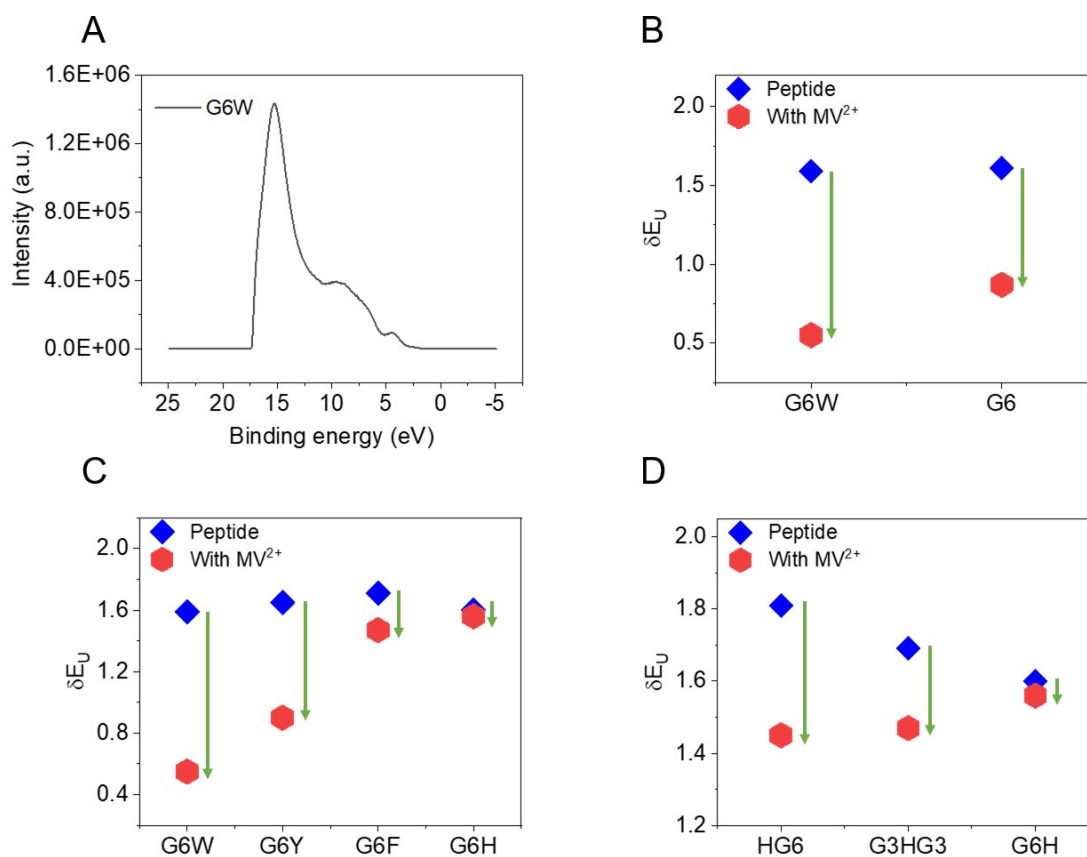
Fig. S11 δE_U values obtained from UPS spectra. (A) Typical UPS spectrum of G6W SAM. (B-D) Trends of δE_U with peptide and peptide-MV^{2+} SAMs. (B) G6W- and G6-based SAMs, (C) Peptide-based SAMs with aromatic amino acid residues on the top and (D) Peptide-based SAMs with His located at the C-terminus, in the middle, and at N-terminus. δE_U is the energy offset of peptide SAM between the highest occupied molecular orbital (HOMO) and Au Fermi energy.
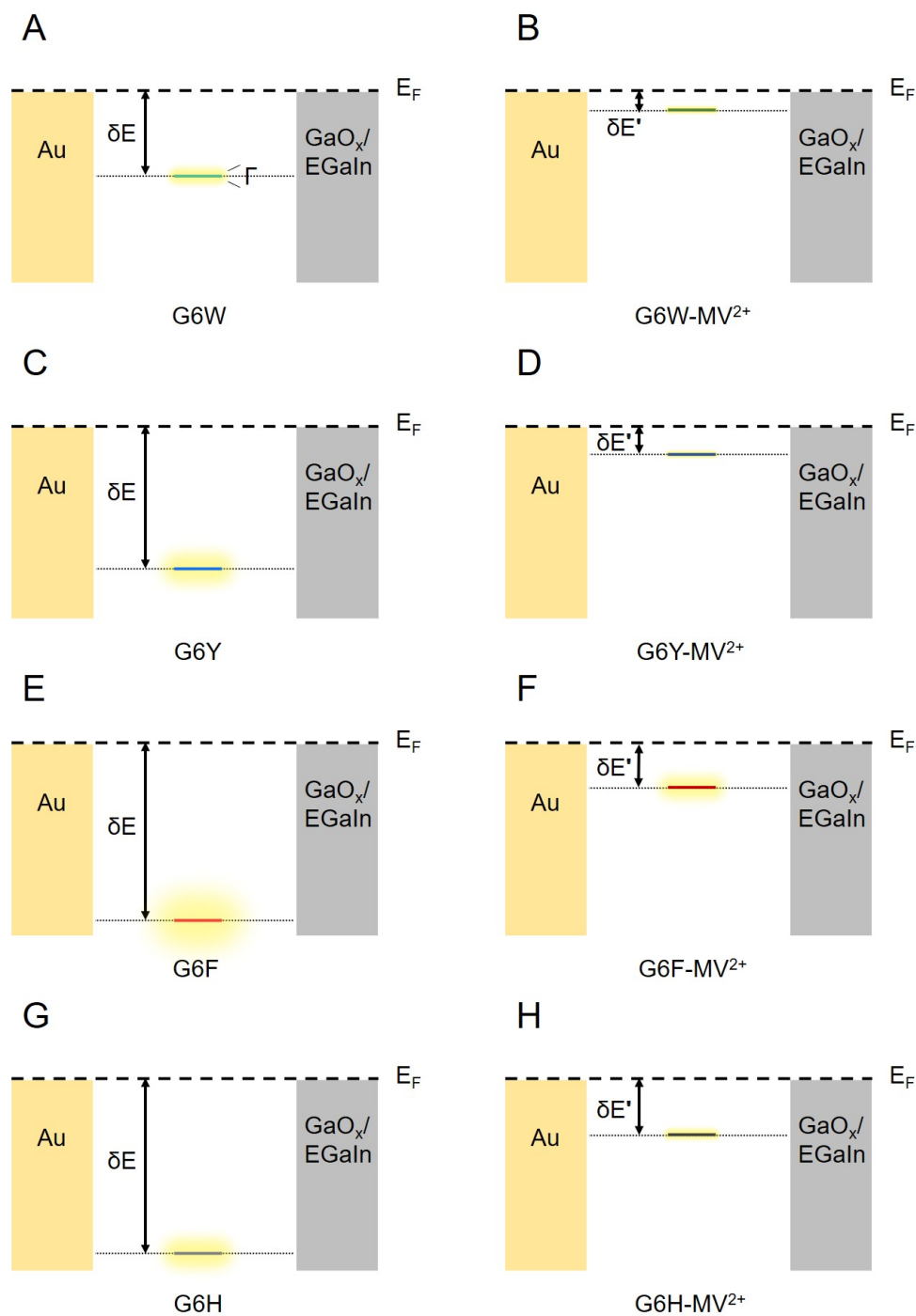
Fig. S12 Schematic energy level diagrams of the peptide-based SAMs with aromatic amino acid residues on the top. (A) G6W, (B) G6W-MV^{2+}, (C) G6Y, (D) G6Y-MV^{2+}, (E) G6F, (F) G6F-MV^{2+}, (G) G6H, and (H) G6H-MV^{2+} SAMs. E_F is the electrodes' Fermi level. δE is the energy barrier. Molecule-electrode coupling (Γ) is highlighted in yellow. δE and $\delta E'$ show the energy barriers of the peptide and peptide-MV^{2+} SAMs, respectively.
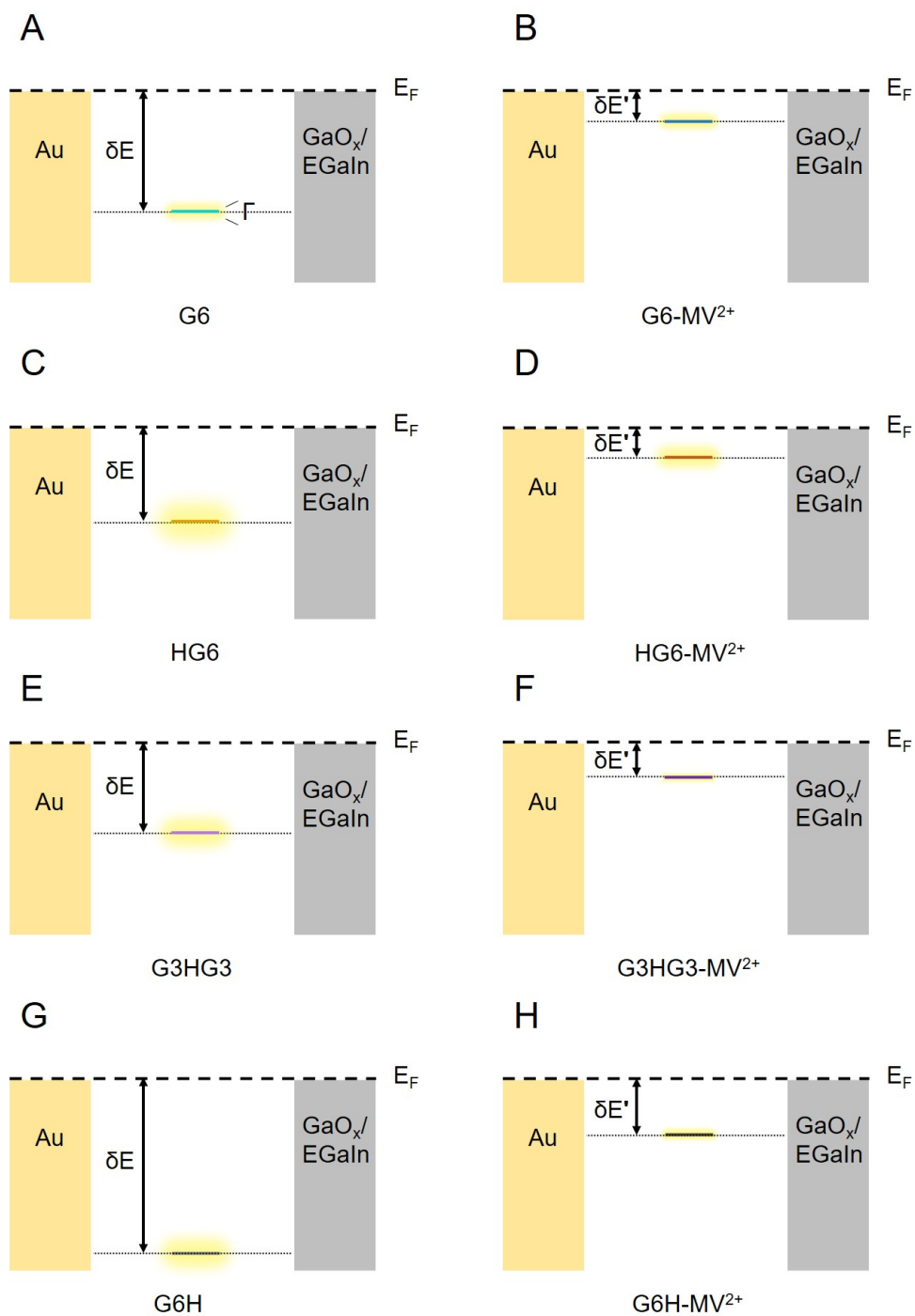
Fig. S13 Schematic energy level diagrams of the peptide-based SAMs with different His-MV^{2+} distances and G6-based SAMs. (A) G6, (B) G6-MV^{2+}, (C) HG6, (D) HG6-MV^{2+}, (E) G3HG3, (F) G3HG3-MV^{2+}, (G) G6H, and (H) G6H-MV^{2+} SAMs. E_F is the electrodes' Fermi level. δE is the energy barrier. Molecule-electrode coupling (Γ) is highlighted in yellow. δE and $\delta E'$ show the energy barriers of the peptide and peptide-MV^{2+} SAMs, respectively.

Table S1 Thickness of peptide SAMs under different conditions determined by ellipsometry. Δ = Thickness $_{\text{Peptide-MV}^{2+}}$ – Thickness $_{\text{Peptide}}$.

	Thickness (Å)		
	Peptide	Peptide-MV^{2+}	Δ
G6W	29.8 ± 1.3	32.9 ± 1.7	3.1
G6Y	31.4 ± 0.8	35.0 ± 1.0	3.6
G6F	28.4 ± 1.6	32.1 ± 0.2	3.7
G6H	31.2 ± 1.8	33.6 ± 1.5	2.4
G3HG3	22.4 ± 0.6	25.4 ± 1.2	3.0
HG6	16.6 ± 0.7	21.6 ± 1.2	5.0
G6	25.7 ± 1.0	30.6 ± 0.9	4.9

Table S2 Absorbance of amide I and II and amide I/II ratios for peptide and peptide-MV^{2+} SAMs.

	Amide I (cm^{-1})	Amide II (cm^{-1})	Amide I/II ratio
G6W	1679	1562	0.34
G6W-MV^{2+}	1678	1562	0.25
G6Y	1666	1562	0.37
G6Y-MV^{2+}	1676	1562	0.45
G6F	1666	1560	0.30
G6F-MV^{2+}	1666	1560	0.35
G6H	1677	1562	0.26
G6H-MV^{2+}	1677	1562	0.18
G3HG3	1676	1554	1.15
G3HG3-MV^{2+}	1676	1554	1.06
HG6	1680	1552	2.03
HG6-MV^{2+}	1678	1550	1.89
G6	1658	1564	0.11
G6-MV^{2+}	1658	1564	0.11

Table S3 Surface coverage of peptide SAMs and MV^{2+} as well as the fraction of MV^{2+}.

	Surface coverage (mol·cm^{-2})		Fraction of MV^{2+} (%)
	Peptide SAMs ($\times10^{-10}$)	MV^{2+} ($\times10^{-11}$)	
G6W	7.02	1.63	2.32
G6Y	13.1	2.68	2.05
G6F	8.06	1.90	2.36
G6H	9.56	1.04	1.09
G3HG3	7.37	6.41	8.70
HG6	2.88	2.17	7.53
G6	7.87	1.85	2.35

Table S4 Zeta potential for peptide SAMs with His located at the C-terminus, in the middle, and at N-terminus.

	Zeta potential (mV)
G6H	-31.0 ± 0.3
G3HG3	-55.0 ± 0.8
HG6	-57.4 ± 0.7

Compared to G3HG3 and HG6 SAMs, the zeta potential of G6H SAM is more positive. For peptide SAMs with His located differently, each of the peptide molecules linked at the gold surface has a carboxyl group and an imidazole group. The surface coverage for G6H, G3HG3, and HG6 SAMs is similar and on the same order of magnitude (Table S3), which means that the surface of peptide SAMs has a comparable number of negatively charged carboxylate groups. The more positive zeta potential for G6H SAM indicates that the imidazole groups in His are positively charged. Furthermore, based on the zeta potential values, the degree of His exposed to the surface is in the trend of G6H > G3HG3 > HG6.

References

1. S. Ikeyama and Y. Amao, *ChemCatChem*, 2017, **9**, 833-838.

2. E. A. Weiss, G. K. Kaufman, J. K. Kriebel, Z. Li, R. Schalek and G. M. Whitesides, *Langmuir*, 2007, **23**, 9686-9694.

3. M. Hegner, P. Wagner and G. Semenza, *Surf. Sci.*, 1993, **291**, 3946.

4. I. Bâldea, *Phys. Rev. B*, 2012, **85**, 035442.

5. X. B. Li, P. A. Cazade, P. Qi, D. Thompson and C. L. Guo, *Chin. Chem. Lett.*, 2023, **34**, 107466.

6. Y. Li, X. B. Li, P. Qi and C. L. Guo, *Chem. Commun.*, 2022, **58**, 6405-6408.

7. C. Guo, X. Yu, S. Refaely-Abramson, L. Sepunaru, T. Bendikov, I. Pecht, L. Kronik, A. Vilan, M. Sheves and D. Cahen, *Proc. Natl. Acad. Sci. U. S. A.*, 2016, **113**, 10785-10790.

8. C. Guo, Y. Gavrilov, S. Gupta, T. Bendikov, Y. Levy, A. Vilan, I. Pecht, M. Sheves and D. Cahen, *Phys. Chem. Chem. Phys.*, 2022, **24**, 28878-28885.